Helmholtz-Zentrum
Geesthacht
Zentrum für Material- und Küstenforschung

Final Draft
of the original manuscript:

Schmutzler, T.; Schindler, T.; Schmiele, M.; Appavou, M.; Lagesa, S.; Kriele, A.; Gilles, R.; Unruh, T.:

The influence of n-hexanol on the morphology and composition of CTAB micelles.

In: Colloids and Surfaces A. Vol. 543 (2018) 56 - 63.
First published online by Elsevier: 21.12.2017

https://dx.doi.org/10.1016/j.colsurfa.2017.12.039

ACCEPTED MANUSCRIPT

The influence of *n*-hexanol on the morphology and composition of CTAB micelles

Tilo Schmutzler[a], Torben Schindler[a], Martin Schmiele[a], Marie-Sousai Appavou[b], Sebastian Lages[a,c], Armin Kriele[d], Ralph Gilles[e], Tobias Unruh[a*]

[a] *Crystallography and Structural Physics, Friedrich-Alexander-Universität Erlangen-Nürnberg, 91058 Erlangen, Germany*

[b] *Forschungszentrum Jülich GmbH, Jülich Centre for Neutron Science (JCNS), Outstation at FRM II, 85747 Garching, Germany*

[c] *MAX IV Laboratory, Lund University, P.O. Box 118, SE-22100 Lund, Sweden*

[d] *German Engineering Materials Science Centre (GEMS), Helmholtz Zentrum Geesthacht (HZG), Max-Plank-Straße 1, 21502 Geesthacht, Germany*

[e] *Heinz Maier-Leibnitz Zentrum (MLZ), Technische Universität München, 85747 Garching, Germany*

Graphical abstract

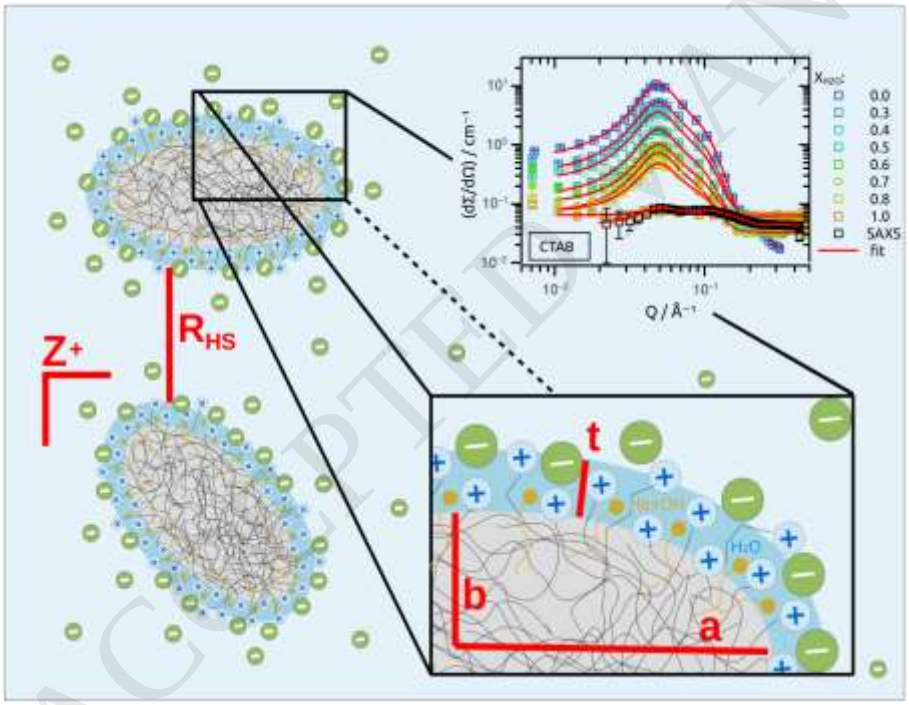

Abstract

The effect of the addition of *n*-hexanol as co-surfactant on the structure of cetyltrimethylammonium bromide (CTAB) micelles has been studied using small-angle X-ray and neutron scattering (SAXS, SANS). Contrast variation neutron scattering experiments were performed to determine the structure of both pure CTAB and *n*-hexanol modified CTAB micelles. The incorporation of *n*-hexanol leads to

ACCEPTED MANUSCRIPT

an elongation of the ellipsoidal CTAB micelles. The scattering length density of the micellar shell linearly depends on the degree of deuteration of the dispersion medium water and revealed the existence of substantial amounts of water in the micellar shell. The water content in the shell increased from 20 vol-% observed for pure CTAB micelles to 44 vol-% found for *n*-hexanol modified CTAB micelles. The amount of *n*-hexanol in the micellar shell was determined by varying the amount of fully deuterated and protonated *n*-hexanol. These experiments revealed a volume fraction of 26 vol-% of *n*-hexanol molecules in the micellar core which equals a molar fraction of 50 % *n*-hexanol within the CTAB micelles. The total composition of micellar core and shell was estimated. The packing density of headgroups, water molecules and bromide ions turned out to drastically increase in *n*-hexanol modified CTAB micelles. These findings contribute to a fundamental understanding of the stabilization mechanism of micelles by alcoholic co-surfactants and the resulting alteration of the morphology and interface composition. These results will facilitate the optimization of processes where CTAB and other comparable surfactants are used as phase transfer catalysts, structure directing agents or stabilizers in colloidal dispersions or emulsions.

Keywords: CTAB micelles; surfactants; co-surfactants; SANS; SAXS

Introduction

The importance of surfactants in various fields of scientific research is predominantly related to their amphiphilic behavior. This property directly leads to numerous applications in catalysis and the stabilization of colloidal emulsions and suspensions..[1][2][3][4][5][6] It is well known, that micelles are capable to catalyze chemical reactions and direct structure forming processes in both hydrophilic and hydrophobic solvents.[7][8][9][10][11] Due to the amphiphilic nature of surfactants, the concentration-dependent formation of self-assembled structures like e.g. micelles, vesicles and liquid crystals is observed besides their molecular disperse distribution in solution.[12]

Cetyltrimethylammonium bromide (CTAB) is one of the most common surfactants and is widely used in the synthesis of inorganic nanoparticles, mesoporous silica and as catalyst in redox reactions.[7][10][13] CTAB forms micelles in water above a critical micelle concentration (cmc) slightly below 0.001 mol/L at room temperature.[14] At higher concentrations, the elliptical micelles become more elongated and rod-like shapes are formed at around 0.3 mol/l.[14][15] It is well known, that short and medium length *n*-alcohols influence these transitions by acting as co-surfactants.[16][17][18][19] Co-surfactants can be described as surfactants which are not capable to form stable micelles on their own. However, these molecules can be incorporated into the micelles by effecting their structure and cmc.[20] *N*-alcohols shorter than *n*-butanol seem to act as co-solvents rather than as co-surfactants and are not predominately incorporated into the micelles.[16]

ACCEPTED MANUSCRIPT

N-alcohols longer than *n*-butanol are only partially soluble in water and thus significantly influence the size and shape of the micelles by getting incorporated into their structure.[21][22]

A lot of work has been done regarding the structure of CTAB micelles.[23][24][25][26] However, the structure modification induced by *n*-alcohols especially at CTAB concentrations significantly higher than the cmc has not been intensively studied. It is known that the addition of *n*-octanol to CTAB dispersions promotes the phase transition towards rod-like micelles whereas methanol has the opposite effect of decreasing the micelle size.[27][28] In addition to the morphology the composition of micellar core and shell changes by the incorporation of alcohols into micelles.[21][29] Small-angle neutron scattering techniques has been successfully conducted to determine the location of certain molecules within complex core-shell structures.[22][30][31][32]

In this work a general approach to determine both morphology and composition of *n*-alcohol-modified CTAB micelles is presented.

The combination of small-angle X-ray (SAXS) and neutron scattering (SANS) is very promising to analyze complex colloidal structures like organic nanocrystals, emulsions and molecular self-assemblies.[33][34][35][36][37][38][39][40]

The results of a combined structural analysis of CTAB and *n*-hexanol modified CTAB micelles using SAXS and contrast variation SANS are presented in this work. The scattering contrast of the micelles in different D_2O/H_2O mixtures could be correlated with the water content in the micellar shell. The results are in accordance with molecular dynamics simulations known from literature.[41][42] The incorporation of *n*-hexanol into CTAB micelles leads to larger, more elongated structures with a much higher amount of water in the shell. These findings will be of importance for numerous applications of CTAB solutions and will help to further improve the properties of such micellar solutions in terms of catalytic activity and morphological selectivity.

Materials and Methods

Tab.1: *Volume fraction of H_2O in D_2O $V_{H2O/D2O}$ to achieve H_2O molar fractions X_{H2O} and corresponding scattering length densities (SLD) for neutrons of the solvent. SLD of H_2O is given for X-rays.*

$V_{H2O/D2O}$	X_{H2O}	SLD / cm^{-2}
∞	1.00	9.42e10 (X-rays)
∞	1.00	-5.59e9
3.00	0.75	1.18e10
2.40	0.71	1.48e10
1.80	0.64	1.92e10
1.20	0.55	2.59e10
0.60	0.38	3.76e10
0.36	0.27	4.52e10
0.00	0.00	6.33e10

ACCEPTED MANUSCRIPT

Cetyltrimethylammonium bromide (CTAB, $C_{19}H_{42}BrN$, > 99 %, Sigma), *n*-hexanol (HexOH, $C_6H_{13}OH$, ≥ 99 %, Sigma-Aldrich) and deuterated *n*-hexanol (*d*-HexOH, $C_6D_{13}OH$, 98%, Eurisotop) were used without further purifications. Aqueous CTAB solutions (0.1 mol/L) were prepared by dissolving corresponding amounts of CTAB in H_2O or D_2O, respectively. To obtain 5 mL of an equimolar mixture of CTAB and *n*-hexanol (CTAB/HexOH, 0.1 mol/L, respectively), 4.875 mL of 0.1 mol/L CTAB solution were mixed with 0.0624 mL of pure *n*-hexanol (c=8.025 mol/L). To correct for the increased volume caused by the addition of *n*-hexanol, 0.0624 mL of 0.2 mol/L CTAB solution was added (4.875 + 2 * 0.0624 = 5) assuming a linear volume increase by mixing the different liquids. To conduct contrast variation SANS experiments, solutions of CTAB (or CTAB/HexOH) in H_2O were mixed with corresponding solutions in D_2O with the volume ratio $V_{H2O/D2O}$. The corresponding mole fractions of H_2O (X_{H2O}) and scattering length densities (SLD) of the solvent are given in Tab.1. The samples for SAXS and SANS were prepared in the Materials Science laboratory which is running in collaboration of the Technical University Munich (TUM) and Helmholtz Zentrum Geesthacht at the Heinz Maier-Leibnitz Zentrum (MLZ) at the FRM II in Garching.

Small-angle X-ray scattering (SAXS)

SAXS data were collected at the SAXS beamline I911-4 at the MAX IV Laboratory (Lund, Sweden) which was equipped with a bent Si (111) crystal (horizontally focusing) and a multilayer mirror for a curved focus in the vertical (R=400 m).[43][44] The experiments were performed at an X-ray wavelength of 0.91 Å and an energy resolution of $\Delta E/E \sim 10^{-3}$. The sample to detector distance (SDD) of 2350 mm allowed to access the *Q*-range of 0.01 – 0.3 $Å^{-1}$. Silver behenate was used as standard to determine the SDD and the coordinates of the beam center on the detector.[45][46] A Pilatus 1M detector (Dectris AG, Switzerland) was used for data acquisition. The SURF setup which allowed simultaneous measurements of SAXS and spectroscopy was used as sample environment.[47] The setup was equipped with a silica glass capillary with a diameter of 2 mm as a flow cell. All measurements were done at 303 K to prevent CTAB precipitation. The FIT2D software was used for azimuthal integration of the raw data.[48] The resulting scattering curves were normalized to incidence flux, transmission and acquisition time. A measurement of pure water was used to subtract the solvent contribution from the sample measurements. The scattering curves were calibrated to absolute scale using the differential scattering cross section of water.[49][50] For the SAXS data modeling the software SASfit was used which employs the Levenberg-Marquardt method for the non-linear least square regression.[51]

Small-angle neutron scattering (SANS)

SANS experiments were performed at the KWS-2 instrument of the Jülich Center for Neutron Science (JCNS) at the Heinz Maier-Leibnitz Zentrum (MLZ) at the FRM II in Garching, Germany.[52] A beam size of 8 x 8 mm^2 at the sample position was chosen and the data were recorded at two SDDs (1.4 m and 8 m, collimation length: 8 m) to gather a *Q*-range from 0.006 $Å^{-1}$ to 0.469 $Å^{-1}$. The wavelength was set to 4.54 Å with a wavelength spread of $\Delta\lambda / \lambda = 20\%$. The data was corrected for

ACCEPTED MANUSCRIPT

background by the measurement of a boron carbide slab. For detector sensitivity correction and the calibration to the absolute scale of the differential scattering cross section the measurement of a polymethylmethacrylat (Plexiglas, 1mm) standard was used. The data reduction was performed using the software QTIKWS.[53] All samples were measured at 308 K to avoid precipitation of CTAB.

Analysis of SAXS / SANS data and fitting model

The scattered intensity I(*Q*) can be expressed in terms of the scattering length density (SLD):

$$I(Q) = FT(\int SLD(r)SLD(r-u)dr) = FT(P(u)) \quad (1)$$

with

$$Q = \frac{4\pi}{\lambda}\sin(\frac{2\theta}{2}) = \frac{2\pi}{d} \quad (2)$$

Here, ***FT*** denotes the Fourier transformation and *P(**u**)* the Patterson function. The modulus of the scattering vector ***Q*** is given in (2). ***Q*** is defined as $\boldsymbol{Q}=\boldsymbol{k}_f-\boldsymbol{k}_i$, where $\boldsymbol{k}_i$ and $\boldsymbol{k}_f$ are the wave vectors of the incident and the scattered waves, respectively. The distance d represents the real space analogue to *Q, λ* the X-ray and neutron wavelength, respectively and 2*θ* the scattering angle. The small-angle approximation leads to the scattered intensity of particles:[54]

$$I(Q) = (\Delta SLD)^2 * N * S(Q) * \int f(R) * [V(R)]^2 * [F(Q,R)]^2 dR \quad (3)$$

$\Delta SLD = SLD_{core} - SLD_{sol}$ is the excess SLD which is given by the SLD of the micelles SLD_{core} and the solvent (water, SLD_{sol}). *S(Q)* denotes the structure factor, *N* the total number of particles, *V(R)* the particle volume and *f(R)* their relative frequency. *F(Q,R)* denotes the form factor amplitude.

For the concentrations used in the present study, CTAB forms ellipsoidal core-shell micelles in water.[26] Thus, the form factor amplitude $F(Q,R)_{ellip}$ can be described by the formula:[51]

$$F(Q,\mu)_{ellip} = (SLD_{core} - SLD_{sh})V_C[\frac{3j_i(x_c)}{x_c}] + (SLD_{sh} - SLD_{sol})V_t[\frac{3j_i(x_t)}{x_t}] \quad (4)$$

with

$$j_i = \frac{\sin(x_i) - x_i\cos(x_i)}{x_i^2},\ (i = c, t) \quad (5)$$

$$x_c = Q\sqrt{a^2\mu^2 + b^2(1-\mu^2)}, x_t = Q\sqrt{(a+t)^2\mu^2 + (b+t)^2(1-\mu^2)} \quad (6)$$

ACCEPTED MANUSCRIPT

$$V_c = \frac{4}{3}\pi ab^2 \quad (7)$$

$$V_t = \frac{4}{3}\pi(a+t)(b+t)^2 \quad (8)$$

The micellar hydrocarbon core with the volume V_c is characterized by the lengths of the semi-axes *a* and *b* and the SLD_{core}. V_t denotes the total volume of the ellipsoidal particles including core and shell. The shell thickness is given by *t* and the scattering contrast results from the difference between the SLD of the shell SLD_{sh} and that of the solvent water SLD_{sol}. A particle size distribution needs to be taken into account since the micelles could not be considered as completely monodisperse. A Gaussian distribution turned out to describe the shell thickness extremely well:

$$f(x) = \frac{A}{c_{gauss}} e^{-\frac{(x-t)^2}{2\sigma^2}} \quad (9)$$

$$c_{gauss} = \sqrt{\frac{\pi}{2}}\sigma\left(1 + erf\left(\frac{t}{\sqrt{2}\sigma}\right)\right) \quad (10)$$

with *A* being the area under the curve and *σ* the standard deviation of the shell thickness *t*. The interactions between CTAB micelles were taken into account by means of a structure factor S(Q):[40]

$$S(Q) = 1 + 4\pi\epsilon\int (g(r) - 1)\frac{sinQr}{Qr} r^2 dr \quad (11)$$

where *ε* is the particle density, *g(r)* the probability to find another particle at a distance *r* from any randomly chosen particle. This probability strongly depends on the interaction potential of the particles. In this work we assumed a screened Coulomb repulsion which was calculated by Hayter and Penfold with a mean spherical approximation.[24][25] This model is applicable for charged micelles in water including the parameters R_{HS} (hard sphere radius of particles), Z^+ (charge of particles), *η* (volume fraction of particles), *T* (sample temperature), [salt] (monovalent salt concentration) and ε_r (dielectric constant of the solvent). R_{HS} represents a measure of the minimal inter-micellar distance. D_2O and H_2O possess almost the same ε_r at room temperature and a value of 71.08 was used for all model calculations.[55][56] Polydispersity and anisotropy of the micelles were not taken into account for the structure factor calculation. The comparison with fits obtained considering the decoupling approach for the structure factor did not result in noteworthy differences (see the supplementary information Tab.SI1, Tab.SI2).[57] With the SLD of the micellar core obtained from data modeling, *η* was calculated using equation (10) and the SLD calculator that is implemented in the SASfit software:[51]

ACCEPTED MANUSCRIPT

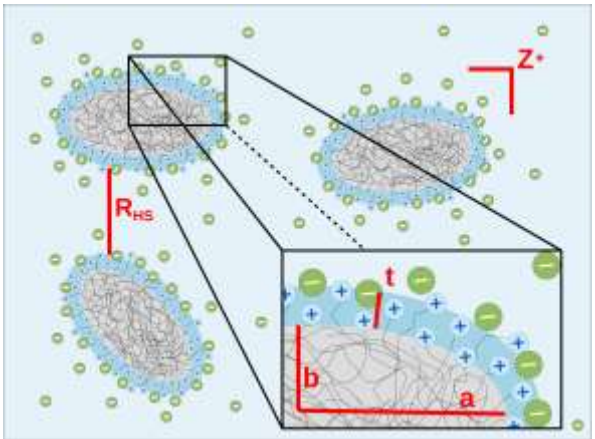

Fig.1: *illustrative representation of the used fitting model to describe the CTAB micelle structure.*

$$\eta = \frac{V_{mic}}{V_{sol}+V_{mic}} = \frac{N_{mic}V_t}{V_{tot}} = \frac{N_{CTAB}V_t}{N_{agg}V_{tot}} = \frac{n_{CTAB}N_AV_t}{N_{agg}V_{tot}}$$

(12)

$$N_{agg} = \frac{\rho_{core}N_AV_c}{M_{core}} = \frac{SLD_{core}*V_c}{b_{core}}$$

(13)

where V_{mic} denotes the total volume of micelles in a certain volume of solvent (V_{sol}) leading to the total volume V_{tot}. Therefore, N_{mic} is the number of micelles within the volume V_{sol} which can be calculated from the total number of CTAB molecules (N_{CTAB}) and the amount of CTAB molecules per micelle (N_{agg}). N_{CTAB} can be calculated from the CTAB concentration of 0.1 mol/L and the Avogadro number (N_A = 6.022x10^{23} mol^{-1}). N_{agg} can also be extracted from the SLD_{core} using the scattering length b_{core} of the core. M_{core} is the molar mass of the part of CTAB molecules which is located in the micelle core. As described in literature,-$C_{13.5}H_{28}$-chains with a molar mass M_{core}=190.36 g/mol located in the core and -$C_{2.5}H_5$-$N(CH_3)_3^+$-head groups with a molar mass of M_{head}=94.18 g/mol in the shell of the micelles were assumed.[15][26] Thus, the micellar shell includes 2.5 “wet” methylene groups in average, plus the trimethylammonium group and bromide counterions. Ionic micelles are not saturated in terms of charge neutrality because not all counterions are bound to the Stern layer.[12]

Tab.2: *Comparison of structural parameters of elliptical core-shell CTAB micelles from literature and this work.*

Major half-axis	Minor half-axis	Shell thickness	source
37.8	20.1	6.5	[26]
40.2	24.0	4.2	[40]
47.2	26.5	6.5	[60]
33.7	27.8	-	[61]
33.0	17.6	7.0	This work

ACCEPTED MANUSCRIPT

An outer, second shell can be considered where solvated bromide ions are accumulated compared to the bulk solution. This shell is described as Gouy-Chapman layer.[12] The micellar core was assumed to resemble a liquid alkane droplet which is supported in literature.[58][59] The model of the micelle structure is systematically depicted in Fig.1 including the most important fitting parameters (red) listed in Tab.3. Despite the high amount of fitting parameters the chosen model turned out to be a good choice since it perfectly describes nine data sets obtained from contrast variation SANS and SAXS experiments for corresponding samples.

Results and Discussion

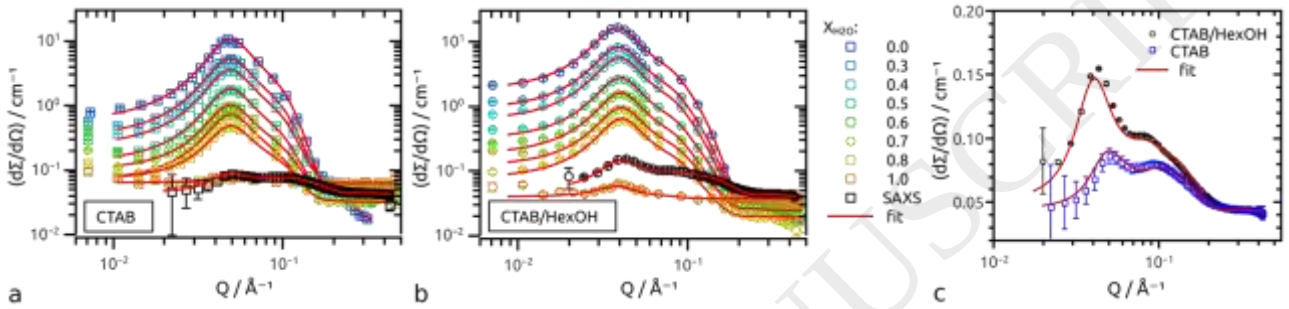

Fig.2: *Contrast variation SANS and SAXS data (black) of 0.1 mol/L CTAB (a) and 0.1 mol/L n-hexanol and CTAB respectively (b) at different H_2O mole fractions (X_{H2O}) in D_2O as solvent resulting in a change of the neutron scattering contrast. The amount of data points in the SANS curves was reduced by a factor of 5 (in SAXS by 2) in behalf of clarity. The SAXS data and fits are separately depicted in c for both CTAB (blue squares) and CTAB/HexOH micelles (black circles). For the same sample all fits (red solid lines) were obtained by simultaneous fitting of all parameters except for R_{HS} and SLD_{shell}.*

To understand the influence of *n*-hexanol incorporated into CTAB micelles, it is crucial to know the structure in their unmodified state. Morphological parameters of CTAB micelles found in literature are summarized in Tab.2.[15][26][40][60][61] Contrast variation SANS experiments in literature proposed an isotope dependency of the CTAB micelle structure. The consequence was that all parameters were fitted separately for each contrast.[26] In this work no isotope dependency on the micelle morphology has been observed and a different approach was chosen. The SASfit software was used to fit the parameters of all data sets simultaneously, except for R_{HS} and SLD_{shell} which exhibited an isotope dependency.[15] These isotope dependency was also verified with SAXS, where R_{HS} was drastically and SLD_{shell} slightly changing by replacing D_2O with H_2O which is documented in the supplementary information (c.f. Fig.SI1). Both, contrast variation SANS and SAXS on absolute scale in combination with simultaneous fitting are necessary to solve the large set of fitting parameters given by the ellipsoidal core-shell form factor *F(Q,R)* and the Hayter-Penfold structure factor *S(Q)*.[24][25] We used the form factor parameters found in literature as starting parameters but introduced a Gaussian distribution of the shell thickness to exactly describe the scattering at high *Q* values (c.f. Fig. 2). The SLD_{core} was chosen such that the mass density of the core ρ_{core} was comparable to liquid alkanes (0.794 g/cm^{-3}) and consistent for neutron and X-ray scattering.[58][59]

ACCEPTED MANUSCRIPT

Tab.3: *Fitting parameters obtained from simultaneous fitting of contrast variation SANS and SAXS data of 0.1 mol/L CTAB and CTAB/HexOH solutions. The shell thickness t is given with the standard deviation σ. a and b are the half-axis of the core-shell ellipsoid with the scattering length densities of core (SLD_{core}). S(Q) includes the distance parameter R_{HS}, the particle charge Z^+, the volume fraction of the micelles η and the free salt concentration [salt]. The packing parameter P was calculated using formula 14.*

X_{H2O}	CTAB	CTAB/HexOH
σ / Å	3.2	3.2
***t* / Å**	7.0	7.0
***a* / Å**	33	62
***b* / Å**	18	18
SLD_{core} **/ cm⁻ ²**	-3.75e09	-4.20e09
SLD_{core} **SAXS / cm⁻ ²**	7.74e10	7.74e10
Z^+	66	85
η / Vol-%	6	7
[salt] / mol/L	2.9e-05	5.5e-05
P	0.37	0.39

The scattered intensity at around 0.1 $Å^{-1}$ was observed to be significantly higher in the case of *n*-hexanol modified CTAB micelles compared to pure CTAB micelles. Accordingly, the modified micelles were found to be more elongated along the semi-axis *a* compared to the unmodified micelles. The semi-axis *b* (*b*=*c* in a biaxial ellipsoid) was not changing with the alcohol modification of the micelles which is in agreement to other micellar systems.[22][29] The summary of all fitting parameters that were independent of the molar fraction of H_2O in H_2O/D_2O mixtures X_{H2O} are summarized in Tab.3 for both: CTAB and CTAB/HexOH micelles. Charge (Z^+) and free salt concentration ([salt]) were fitted simultaneously to consistently fit the data at low Q. Since these two parameters depend on each other, their reliability should be proven using complementary techniques to discuss them in more detail. However, in this study, the morphology of the micelles was of the main interest.

The morphological transition into more elongated micelles caused by the incorporation of *n*-hexanol was already proposed in literature but not quantified.[62] The increase of the micelle size is consistent with spectroscopy studies on the influence of *n*-octanol and *n*-nonanol on CTAB micelles.[20] An estimation of the micelle morphology can be given by the well known packing parameter *P*:[63]

$$P = \frac{V_c}{A * L_{chain}} = 1 - \frac{L_{chain}}{2}\left(\frac{1}{a} + \frac{1}{b}\right) + \frac{L^2_{chain}}{3ab} \quad (14)$$

Tab.4: *Fitting parameters obtained from simultaneous fitting of contrast variation SANS and SAXS data of 0.1 mol/L CTAB and CTAB/HexOH solutions with certain mole fractions X_{H2O} of H_2O in H_2O/D_2O mixtures. X_{H2O} in the SAXS measurement was 1.0. The scattering length densities of the shell (SLD_{shell}) and the distance parameter R_{HS} of S(Q) were fitted in dependence of X_{H2O}.*

	CTAB		CTAB / HexOH	
X_{H2O}	SLD_{shell} / cm⁻ ²	R_{HS} / Å	SLD_{shell} / cm⁻ ²	R_{HS} / Å
0	1.03e10	33.5	2.80e10	47.1
0.27	9.03e09	33.9	2.06e10	46.1
0.38	9.36e09	33.8	1.80e10	45.8
0.55	6.02e09	33.6	1.29e10	45.0
0.64	5.39e09	33.8	9.44e09	44.7

ACCEPTED MANUSCRIPT

0.71	2.27e09	33.5	8.43e09	44.4
0.75	2.51e09	33.5	6.85e09	44.2
1.00	-3.01e09	33.0	-3.10e09	44.7
SAXS	1.02e11	34.7	1.03e11	44.0

where A is the surface area of the amphiphile, V_c the volume of the micellar core and L_{chain} the length of the hydrophobic tail within the core. For ⅓ < P < ½ one would expect a transition from spherical to rod-like micelles which is in agreement to the results of CTAB micelles (P = 0.37) and CTAB/HexOH micelles (P = 0.39, c.f. Tab.3) where the larger value represents a more pronounced elongation of the micelles which supports the small-angle scattering results. The second part of equation 14 was used to estimate P since the semi-axes a and b of the micelles can directly be taken from the contrast variation SANS (and SAXS) fits.

The increased volume of *n*-hexanol modified micelles led to slightly different values for the parameters of $S(Q)$ (c.f. Tab.3 and Tab.4). We noticed that the SLD_{shell} and the R_{HS} does obviously depend on X_{H2O}. The X_{H2O} dependent values for SLD_{shell} and R_{HS} are given in Tab.4.

To consider this in the simultaneous fitting procedure all parameters (except for R_{HS} and SLD_{shell}) were defined as global parameters in each data set which is possible in the SASfit-Software.[51] Correspondingly, these parameters were fitted simultaneously for all data sets. R_{HS} and SLD_{shell} were fitted not depending on the other data sets at the same time.

It is well known that the ratio of the required space for the head group and tail group mainly determines the morphology of the formed micelles.[63] If the required space for the head group becomes smaller, the deviation from spherical shape towards worm-like shaped micelles becomes more expressed.[22][29][64] Thus, the incorporation of smaller, uncharged head groups – in this case hydroxyl groups compared to trimethylammonium groups - leads to a decrease of the head group repulsion. Consequently, the formation of more elongated CTAB micelles by the incorporation of *n*-hexanol is favorable. Additionally, the morphology of the micelles is temperature dependent where elongation is preferred at lower temperatures which is documented in the supplementary information (c.f. Fig.SI1).

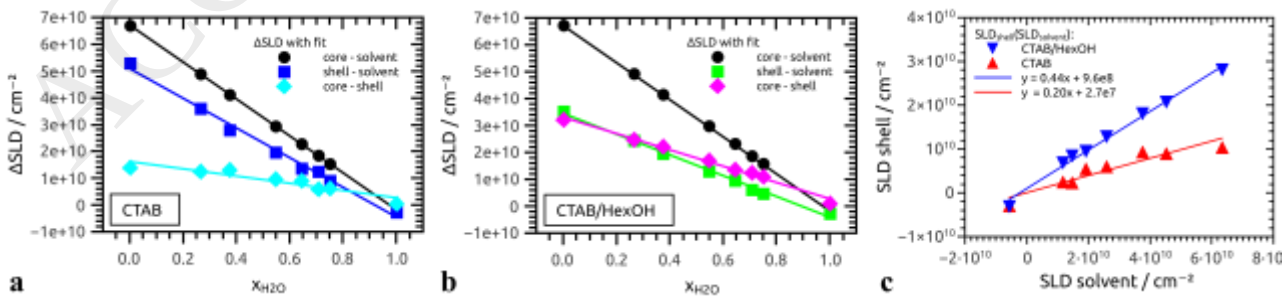

Fig.3: *Scattering contrast (ΔSLD) including linear fits (solid lines) between micelle core and solvent (black circles) of CTAB micelles (a) and CTAB/HexOH micelles (b) in different H_2O/D_2O mixtures with X_{H2O} as H_2O mole fraction. The contrast between micelle shell and core (diamonds) shows a linear dependency with X_{H2O} which indicates the incorporation of solvent molecules into the shell. The slope of SLD_{shell} in dependence of SLD_{sol} (c) gives the amount of water in the micelle shell in both CTAB (red triangles, 20 vol-%) and*

ACCEPTED MANUSCRIPT

CTAB/HexOH (blue triangles, 44 vol-%) micelles.

A quantitative evaluation of the contrast variation experiments revealed that the contrast between the micellar core and the shell is changing linearly with increasing X_{H2O} (c.f. Fig. 3a). Hence, the scattering length densities cannot be constant for both with changing X_{H2O}. The incorporation of water into the micellar shell would explain the scattering contrast dependency between the micellar core and the shell on X_{H2O} and was already predicted by theory.[41][42] For the *n*-hexanol modified CTAB micelles the scattering contrast between micellar shell and core was found to decrease even steeper with higher X_{H2O} (c.f. Fig. 3b). This behavior clearly indicates that the water content in the shell of the *n*-hexanol modified

micelles is significantly higher compared to unmodified CTAB micelles.

In this study the amount of water within the shell of the micelles was estimated by correlating the SLD_{shell} with the SLD of the respective H_2O/D_2O mixture (SLD_{sol}). By plotting the SLD_{shell} as a function of the SLD_{sol}, a linear dependency was obtained (c.f. Fig. 3c) which could be fitted with the parameters given in the supplementary information (Tab.SI3). The linear slope was used to quantify the water content within the shell. No water within the micellar shell would lead to a slope of zero whereas a slope of one would indicate a shell of pure water. In this way a quantification of the water amount in the shell can be obtained. For pure CTAB micelles approximately 20 Vol-% of water were found within the shell, whereas a water content of 44 Vol-% was observed for *n*-hexanol modified micelles. In this approach it has been assumed that the hydroxyl groups of *n*-hexanol molecules are located in the micellar shell whereas the alcohol chain is predominantly located in the hydrophobic core. The assumption that the hydroxyl head groups of *n*-hexanol promote the solvation of the micellar shell by enabling the enhanced formation of hydrogen bonds is in accordance with the experimental results.

This effect might increase the thermodynamic stability of *n*-hexanol modified CTAB micelles compared to pure CTAB micelles. Thus, the formation of micelles is more favorable than forming solid, crystalline CTAB at the given temperature and CTAB concentration. Indeed, the solubility of CTAB is drastically increased by the addition of *n*-hexanol.

Tab.5: *Fitting Parameters obtained from simultaneous fitting of SANS data from mixtures of 0.1 mol/L CTAB/n-hexanol and CTAB/fully deuterated n-hexanol solutions in D_2O with different mole fractions X_{dHexOH} of deuterated n-hexanol. Nomenclature is similar to Tab.4.*

X_{dHexOH}	SLD_{core} / cm^{-2}	SLD_{shell} / cm^{-2}	R_{HS} / Å
0	-4.20e09	2.80e10	48.3
0.04	-3.83e09	2.81e10	48.2
0.30	9.70e08	2.88e10	47.9
0.55	3.64e09	2.98e10	47.5
1.00	1.07e10	3.24e10	46.9

ACCEPTED MANUSCRIPT

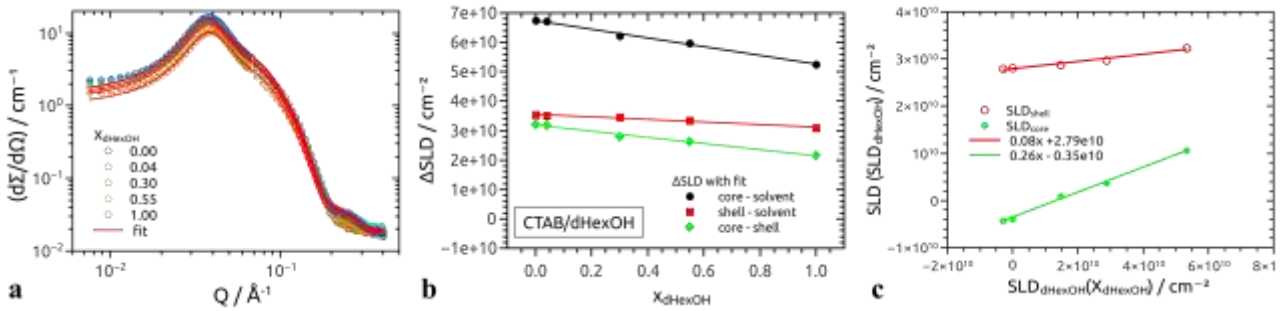

Fig.4: *SANS data including fits (red, solid lines) of CTAB/HexOH micelles in D_2O in dependence of the ratio of deuterated and undeuterated n-hexanol (X_{dHexOH}). Scattering contrast (ΔSLD) including linear fits (solid lines) between micelle core and solvent ($\Delta SLD_{sol\text{-}core}$, black circles), shell and solvent ($\Delta SLD_{sol\text{-}shell}$, red squares) and core and shell ($\Delta SLD_{shell\text{-}core}$, green diamonds) are depicted in b. All three contrasts change linearly with X_{dHexOH} which indicates the incorporation of n-hexanol molecules into the micellar core and shell, respectively. Plotting SLD_{shell} and SLD_{core} in dependence of SLD_{dHexOH} (c) and fitting the linear dependency leads to the amount of n-hexanol molecules in the micellar core (26 %) and shell (8%) of CTAB/HexOH micelles.*

To prove that *n*-hexanol molecules are indeed incorporated in both the micelle core and the shell, we performed contrast variation SANS experiments, replacing protonated *n*-hexanol with fully deuterated *n*-hexanol resulting in the mole fraction of deuterated *n*-hexanol X_{dHexOH}. Three mixtures with different X_{dHexOH} were used. The resulting scattering curves were fitted using the parameters of F(Q,R) and S(Q) depending on X_{dHexOH} given in Tab. 5. The variation of both the SLD_{shell} and the SLD_{core} was necessary to yield reasonable fitting results for the SANS data (c.f. Fig. 4a). The SLD_{shell} and the SLD_{core} increased linearly as a function of X_{dHexOH} (c.f. Fig. 4b). Thus, the scattering contrast between the solvent and the shell ($\Delta SLD_{sol\text{-}shell}$), the solvent and the core ($\Delta SLD_{sol\text{-}core}$) and the shell and the core ($\Delta SLD_{shell\text{-}core}$) decreased linearly with increasing X_{dHexOH}, respectively (c.f. Fig. 4b). These results clearly prove the presence of *n*-hexanol in both the micelle core and the shell. The change of the SLD_{core} is more pronounced compared to the one of SLD_{shell}. Assuming that the hydrocarbon chain of *n*-hexanol is predominantly located in the micelle core leads to a qualitative agreement with the experimental data.

Tab.6: *Length L_{chain} and volume V_{chain} of the hydrophopic parts of the CTAB and hexanol in CTAB and CTAB/HexOH micelles and the respective head group volume of one molecule V_{head} calculated from known literature values.[15] Micellar core V_c, shell V_{sh} and total volume V_t of the micelles were calculated from the values given in Tab.3. The number of amphiphilic molecules within one micelle N_{agg} calculated using formula 13 is in accordance to the ratio of V_c / V_{chain}. The amount of bromide ions in the shell was calculated as the difference from N_{agg} and Z^+ (c.f. Tab.3). The volume fractions of the headgroups Vol-%$_{head}$ and bromide ions Vol-%Br^- is given for the shell and the hydrocarbon chain volume fraction Vol-%$_{chain}$ for the micellar core.*

parameter	CTAB	CTAB-HexOH		
formula (*chain* - [head])	$CH_3(CH_2)_{12.5}$ - $[(CH_2)_{2.5}N(CH_3)_3]$	$CH_3(CH_2)_{12.5}$ - $[(CH_2)_{2.5}N(CH_3)_3]$	average	$CH_3(CH_2)_4$ - $[CH_2OH]$
L_{chain} / nm	1.93	1.93	1.27	0.62
V_{chain} / nm³	0.39	0.39	0.28	0.16
V_{head} / nm³	0.17	0.17	-	0.06
V_c / nm³	42.8	-	79.8	-
V_{sh} / nm³	58.6	-	93.8	-
V_t / nm³	101.4	-	173.6	-
V_c / V_{chain}	110	144	289	144

ACCEPTED MANUSCRIPT

N_{agg}	107	146	292	146
N_{Br^-}	44	-	59	-
Vol-$\%_{head}$ in shell	32	26	35	9
Vol-$\%_{Br^-}$ in shell	2.9	-	2.5	-
Vol-$\%_{chain}$ in core	100	71	100	29

To quantify the amount of *n*-hexanol in both: the micellar core and shell, the fitted SLDs were plotted as a function of the theoretical SLDs of mixtures of protonated *n*-hexanol and fully deuterated *n*-hexanol with a given X_{dHexOH} (c.f. Fig. 4c) that were calculated using the SASfit software. Hence, the linear slope depends on the volume fraction of *n*-hexanol molecules in the respective part of the micelle. A volume fraction of 26 vol-% of *n*-hexanol has been evaluated for the micellar core. This value is consistent to the assumption of an equimolar ratio of *n*-hexanol and CTAB molecules within the micelles which is in agreement to the initial concentration of both compounds in solution. The resulting structure model is schematically represented in Fig.5. The volume of the hydrocarbon chains of CTAB ($C_{12.5}H_{25}$) and *n*-hexanol (C_5H_{11}) within the micellar core (V_{chain}, c.f. Tab.6)

can be calculated using the Volume of CH_3 and CH_2 groups to estimate a theoretical volume percentage of 29 vol-% of *n*-hexanol molecules in an equimolar CTAB and *n*-hexanol containing micellar core.[15] The number of amphiphilic molecules within one micelle (N_{agg}) can be calculated using formula 13 or the quotient of the micellar core volume and V_{chain}. Accordingly, these two methods lead to a total amount of approximately 110 CTAB molecules in pure CTAB micelles and 146 CTAB and 146 alcohol molecules in *n*-hexanol modified CTAB micelles.

The evaluation of the volume fraction of *n*-hexanol in the shell yielded 8 vol-% (c.f. Fig. 4c) which is in agreement to the theoretical value of 9 vol-% (c.f. Tab.6) calculated using:

$$Vol-\%_{head} = \frac{N_{agg} * V_{head}}{V_{sh}} * 100 \quad (16)$$

The volume fraction of CTAB head groups $[(CH_2)_{2.5}N(CH_3)_3]$ can be calculated comparably which yielded a theoretical value of 32 vol-% in the shell of CTAB and 26 vol-% in *n*-hexanol modified CTAB micelles. The number of bromide ions within the micellar shell N_{Br^-} which is given by the difference of N_{agg} and the charge of one micelle (Z^+, c.f. Tab.3) can be used to estimate the volume fraction of bromide ions Vol-$\%_{Br^-}$ within the shell comparably to Vol-$\%_{head}$ and is around 3 vol-% for both micelles. However, these values are a rough estimation, since Z^+ was fitted simultaneously to the unbound bromide concentration within the solution. These values depend on each other and should be validated by other methods to yield reliable values for the amount of bromide ions in the micellar shell. Nevertheless, a packing density can be given by these estimations which yield to 0.49 in CTAB micelles which is comparable to a primitive packing (0.52) and 0.76 in *n*-hexanol modified CTAB micelles which resembles a close packing (ccp, 0.74).[65]

ACCEPTED MANUSCRIPT

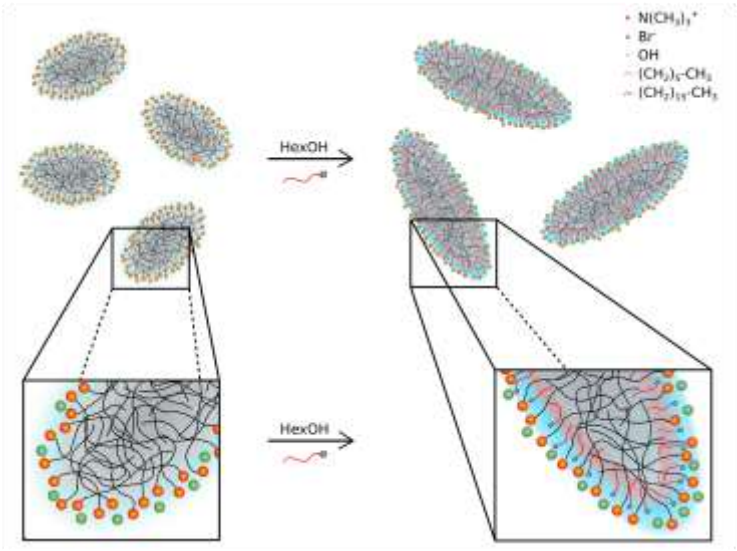

Fig.5: *schematic illustration of the influence of n-hexanol (red) incorporation into CTAB micelles. The ellipsoidal CTAB micelles (left) become more elongated by the modification with n-hexanol (right) and show higher amounts of water in the shell (blue). The n-hexanol molecules are supposed to be located in the hydrophobic core with the hydroxyl group located in the hydrophilic shell.*

The determination of the location of the alcohol molecules and the variation of the composition of the distinct parts of the micelles described above demonstrates the immense versatility of SANS. Since the SLD_{shell} of a core-shell structure changes if the shell is penetrate with solvent molecules, a certain scattering contrast cannot be matched to quantify the amount of a certain compound within the structure as it was done in other studies.[31][22] For the same reason the simple variation of SLD_{sol} cannot be used to completely reveal the composition of the micelles as it has been done for other systems.[30][66] However, as it is shown above the contrast of the solvent and the contrast of both micellar core and shell can be varied to gain a complete picture of the morphology and composition in the described system.[67]

Conclusion

Location and amount of a short-chain alcohol molecule within CTAB micelles were determined unambiguously using small-angle scattering techniques. The incorporation of *n*-hexanol into CTAB micelles leads to the formation of more elongated, ellipsoidal micelles (c.f. Fig. 5). The alteration of the CTAB micelle morphology initiated by the addition of *n*-hexanol is remarkable and might be of interest for applications where CTAB is used as structure directing and stabilizing agent like in gold nanoparticle or mesoporous silica synthesis.[8][10][13]

The incorporation of *n*-hexanol molecules does not only affect the morphology of the micelles but also their internal structure. The amount of water in the hydrophilic shell drastically increases for micelles with incorporated *n*-hexanol. The enhanced solvation of the micelles might be one reason for the increased solubility of CTAB in water by the addition of *n*-hexanol. Additionally, the packing density of water, headgroup molecules and bromide ions within the micellar shell increases drastically by the incorporation of *n*-hexanol. These findings will enable the use of highly

ACCEPTED MANUSCRIPT

concentrated CTAB solutions at lower temperatures because of the drastically increased solubility of CTAB in water. Additionally the exact composition of the water-CTAB interface modified by *n*-hexanol might be of interest in many other scientific fields where surfactants are used as phase transfer catalyst. The phase transfer properties should be drastically influenced by a higher water content and packing density within the interface.

Acknowledgements

The authors would like to acknowledge the funding of the Deutsche Forschungsgemeinschaft (DFG) through the Cluster of Excellence "Engineering of Advanced Materials" (EAM), the research training group 1896 "In Situ Microscopy with Electrons, X-rays and Scanning Probes" and the funding for the SAXS instruments (INST 90/825-1 FUGG, INST 90/751-1 FUGG, INST 90/827-1 FUGG).

References

[1 H. Elworthy, A. T. Florence, C. B. Macfarlane, Solubilization by Surface Active Agents, Chapman and Hall, London, 1968.

[2 Cordes, ed., Reaction Kinetics in Micelles, Plenum Press, New York, 1973.

[3 Schmiele, T. Schindler, T. Unruh, S. Busch, H. Morhenn, M. Westermann, F. Steiniger, A. Radulescu, P. Lindner, R. Schweins, P. Boesecke, Structural characterization of the phospholipid stabilizer layer at the solid-liquid interface of dispersed triglyceride nanocrystals with small-angle x-ray and neutron scattering, Phys. Rev. E 87 (2013) 062316.

[4 Schmiele, S. Busch, H. Morhenn, T. Schindler, T. Schmutzler, R. Schweins, P. Lindner, P. Boesecke, M. Westermann, F. Steiniger, S.S. Funari, T. Unruh, *Structural Characterization of Lecithin-Stabilized Tetracosane Lipid Nanoparticles. Part I: Emulsions, J. Phys. Chem. B 120 (*2016) 5505–5512.

[5 Schmiele, S. Busch, H. Morhenn, T. Schindler, T. Schmutzler, R. Schweins, P. Lindner, P. Boesecke, M. Westermann, F. Steiniger, S.S. Funari, T. Unruh, *Structural Characterization of Lecithin-Stabilized Tetracosane Lipid Nanoparticles. Part II: Suspensions, J. Phys. Chem. B 120 (2016)* 5513–5526.

[6 Damm, D. Segets, G. Yang, B.F. Vieweg, E. Spiecker, W. Peukert, Shape Transformation Mechanism of Silver Nanorods in Aqueous Solution, Small 7 (2011) 147-156.

[7 Pal, S. De, N.R. Jana, N. Pradhan, A.E. Beezer, J.C. Mitchell, Organized Media as Redox Catalysts, Langmuir 14 (1998) 4724-4730.

[8 Pileni, The role of soft colloidal templates in controlling the size and shape of inorganic nanocrystals, Nat. Mater. 2 (2003) 145-150.

[9 Entezari, A.A. Shameli, Phase-transfer catalysis and ultrasonic waves I. Cannizzaro reaction, Ultrason. Sonochem. 7 (2000) 169-172.

[10 Murphy, T.K. Sau, A. Gole, C.J. Orendorff, Surfactant-Directed Synthesis and Optical Properties of One-Dimensional Plasmonic Metallic Nanostructures, MRS Bull. 30 (2005) 349-355.

[11 Taleb, C. Petit, M.P. Pileni, Synthesis of Highly Monodisperse Silver Nanoparticles from AOT Reverse Micelles: A Way to 2D and 3D Self-Organization, Chem. Mater. 9 (1997) 950-959.

ACCEPTED MANUSCRIPT

[12 Fisher, D.G. Oakenfull, Micelles in Aqueous Solution, **Chem. Soc. Rev.** 6 (1977) 25-42.

[13 Kresge, M.E. Leonowicz, W.J. Roth, J.C. Vartuli, J.S. Beck, Ordered mesoporous molecular sieves synthesized by a liquid crystal template mechanism, Nature 359 (1992) 710-712.

[14 Ekwall, L. Mandell, P. Solyom, The Aqueous Cetyl Trimethylammonium Bromide Solutions, J. Colloid Interface Sci.33 (1971) 519-528.

[15 Berr, R.R.M. Jones, J.S. Johnson Jr., Effect of Counterion on Size and Charge of Alkyltrimethyl-ammonium Halide Micelles as a function of Chain Length and Concentration As Determined by Small-Angle Neutron Scattering, J. Phys. Chem. 96 (1992) 5611-5614.

[16 Zana, Aqueous surfactant-alcohol systems: A review, Adv. Colloid Interface Sci. 57 (1995) 1-64.

[17 Mitra, B.K. Paul, S.P. Moulik, Phase behavior, interfacial composition and thermodynamic properties of mixed surfactant (CTAB and Brij-58) derived w/o microemulsions with 1-butanol and 1-pentanol as cosurfactants and n-heptane and n-decane as oils, J. Colloid Interface Sci. 300 (2006) 755-764.

[18 Palazzo, F. Lopez, M. Giustini, G. Colafemmina, A. Ceglie, Role of the Cosurfactant in the CTAB/Water/n-Pentanol/n-Hexane Water-in-Oil Microemulsion. 1. Pentanol Effect on the Microstructure, J. Phys. Chem B 107 (2003) 1924-1931.

[19 Ekwall, L. Mandell, K. Fontell, The Cetyhrimethylammonium Bromide-Hexanol-Water System, J. Colloid Interface Sci. 24 (1969) 639-646.

[20 Dubey, CTAB aggregation in solutions of higher alcohols: Thermodynamic and spectroscopic studies, J. Mol. Liq. 184 (2013) 60-67.

[21 Zana, Effect of Medium Chain-Length Alcohols on the Micelles of Tetradecyltrimethylammonium Bromide, J. Colloid Interface Sci. 101 (1984) 587-590.

[22 Moeller, P. Lang, G.H. Findenegg, Location of Butanol in Mixed Micelles with Alkyl Glucosides Studied by SANS, J. Phys. Chem. B 102 (1998) 8958-8964.

[23 Aswal, P.S. Goyal, Selective counterion condensation in ionic micellar solutions, Phys. Rev. E 67 (2003) 051401.

[24 Hayter, J. Penfold, An analytic structure factor for macroion solutions, Mol. Phys. 42 (1981) 109-118.

[25 Hayter, J. Penfold, Determination of micelle structure and charge by neutron small-angle scattering, Colloid Polym. Sci. 261 (1983) 1022-1030.

[26 Berr, Solvent Isotope Effects on Alkyltrimethylammonium Bromide Micelles as a Function of Alkyl Chain Length, J. Phys. Chem. 91 (1987) 4760-4765.

[27 Desai, D. Varade, J. Mata, V. Aswal, P. Bahadur, Colloids Surf. A 259 (2005) 111-115.

[28 Anderson, J.E. Martin, J.G. Odinek, P.P. Newcomer, Chem. Mater. 10 (1998) 1490-1500.

[29 Moeller, P. Lang, G.H. Findenegg, U. Keiderling, Micellar solutions of octyl monoglucoside in the presence of butanol: A small angle and light scattering study, Ber. Bunsenges. Phys. Chem. 101 (1997) 1121-1128.

[30 Brasher, E.W. Kaler, A Small-Angle Neutron Scattering (SANS) Contrast Variation Investigation on Aggregate Composition in Cationic Surfactant Mixtures, Langmuir 12 (1996) 6270-6276.

ACCEPTED MANUSCRIPT

[31 Schindler, M. Schmiele, T. Schmutzler, T. Kassar, D. Segets, W. Peukert, A. Radulescu, A. Kriele, R. Gilles, T. Unruh, A Combined SAXS/SANS Study for the in Situ Characterization of Ligand Shells on Small Nanoparticles: The Case of ZnO, Langmuir 31 (2015) 10130-10136.

[32 Schindler, T. Schmutzler, M. Schmiele, W. Lin, D. Segets, W. Peukert. M.-S. Appavou, A. Kriele, R. Gilles, T. Unruh, Changes within the stabilizing layer of ZnO nanoparticles upon washing, J. Colloid Interface Sci. 504 (2007) 356-362.

[33 Schmiele, T. Schindler, M. Westermann, F. Steiniger, A. Radulescu, A. Kriele, R. Gilles, T. Unruh, Mesoscopic Structures of Triglyceride Nanosuspensions Studied by Small-Angle X-ray and Neutron Scattering and Computer Simulations, J. Phys. Chem. B 118 (2014) 8808-8818.

[34 Schmiele, S. Gehrer, M. Westermann, F. Steiniger, T. Unruh, Formation of liquid crystalline phases in aqueous suspensions of platelet-like tripalmitin nanoparticles, J. Chem. Phys. 140 (2014) 214905.

[35 Gómez-Grana, F. Hubert, F. Testard, A. Guerrero-Martinez, I. Grillo, L.M. Liz-Marzán, O. Spalla, Surfactant (Bi)Layers on Gold Nanorods, Langmuir 28 (2012) 1453-1459.

[36 Fratzl, Small-angle scattering in materials science – a short review of applications in alloys, ceramics and composite materials, J. Appl. Cryst. 36 (2003) 397-404.

[37 Stuhrmann, Small-angle scattering and its interplay with crystallography, contrast variation in SAXS and SANS, Acta Cryst. A 64 (2008) 181-191.

[38 Roche, M. Pineri, R. Duplessix, A.M. Levelut, Small-angle scattering studies of nafion membranes, J. Polym. Sci., Polym. Phys. Ed. 19 (1981) 1-11.

[39 Millett, S. Doniach, K.W. Plaxco, Toward a taxonomy of the denatured state: Small angle scattering studies of unfolded proteins, Adv. Protein Chem. 62 (2002) 241-262.

[40 Aswal, P.S. Goyal, H. Amenitsch, S. Bernstorff, Counterion condensation in ionic micelles as studied by a combined use of SANS and SAXS, Pramana 63 (2004) 333-338.

[41 Bagchi, Water Dynamics in the Hydration Layer around Proteins and Micelles, Chem. Rev. 105 (2003) 3197-3219.

[42 Pal, B. Bagchi, S. Balasubramaian, Hydration Layer of a Cationic Micelle, C_{10}TAB: Structure, Rigidity, Slow Reorientation, Hydrogen Bond Lifetime, and Solvation Dynamics, J. Phys. Chem. B 109 (2005) 12879-12890.

[43 Mammen, T. Ursby, M. Thunnissen, J. Als-Nielsen, Bent Diamond Crystals and Multilayer Based Optics at the new 5-Station Protein Crystallography Beamline 'Cassiopeia' at MAX-lab, AIP Conf. Proc. 704 (2004) 808-811.

[44 Labrador, Y. Cerenius, C. Svenssson, K. Theodor, T. Pivelic, The yellow mini-hutch for SAXS experiments at MAX IV Laboratory, J. Phys.: Conf. Ser. 425 (2013) 072019.

[45 Huang, H. Toraya, T.N. Blanton, Y. Wu, X-ray powder diffraction analysis of silver behenate, a possible low-angle diffraction standard, J. Appl. Crystallogr. 26 (1993) 180-184.

[46 Gilles, U. Keiderling, A. Wiedenmann, Silver behenate powder as a possible low-angle calibration standard for small-angle neutron scattering, J. Appl. Cryst. 31 (1998) 957-959.

[47 Haas, T.S. Pivelic, C. Dicko, Combined SAXS/UV-vis/Raman as a Diagnostic and Structure Resolving Tool in Materials and Life Sciences Application, J. Phys. Chem. B 118 (2014) 2264-2273.

ACCEPTED MANUSCRIPT

[48 Hammersley, S.O. Svensson, M. Hanfland, A.N. Fitch, D. Haeusermann, Two-Dimensional Detector Software: From Real Detector to Idealised Image or Two-Theta Scan, High Pressure Res. 14 (1996) 235-248.

[49 Dreiss, K.S. Jack, A.P. Parker, On the absolute calibration of bench-top small-angle X-ray scattering instruments: a comparison of different standard methods, J. Appl. Crystallogr. 39 (2006) 32-38.

[50 Fan, M. Degen, S. Bendle, N. Grupido, J. Ilavsky, The Absolute Calibration of a Small-Angle Scattering Instrument with a Laboratory X-ray Source, J. Phys.: Conf. Ser. 247 (2010) 012005.

[51 Breßler, J. Kohlbrecher, A.F. Thünemann, SASfit: a tool for small-angle scattering data analysis using a library of analytical expressions, J. Appl. Crystallogr. 48 (2015) 1587-1598.

[52 Radulescu, V. Pipich, H. Frielinghaus, M.-S. Appavou, KWS-2, the high intensity / wide Q-range small-angle neutron diffractometer for soft-matter and biology at FRM II, J. Phys.: Conf. Ser. 351 (2012) 012026.

[53 Centre for Neutron Science (JCNS), Vitaly Pipich, http://iffwww.iff.kfa-juelich.de/~pipich/dokuwiki/doku.php/ qtikws, 2017 (accessed 4 December 2017)

[54 A. Feigin, D. I. Svergun, Structure Analysis by Small-Angle X- ray and Neutron Scattering; Plenum Publishing Corporation, New York, 1987.

[55 Malmberg, A.A. Maryott, Dielectric Constant of Water from 0 to 100 C, J. Res. Natl. Bur. Stand. 56 (1956) 1-8.

[56 Malmberg, Dielectric Constant of Deuterium Oxide, J. Res. Natl. Bur. Stand. 60 (1958) 609-612.

[57 Kotlarchyk, S.-H. Chen, Analysis of small angle neutron scattering spectra from polydisperse interacting colloids, J. Chem. Phys. 79 (1983) 2461-2469.

[58 Khuanga, B. K. Selinger, R. McDonald, A study of surfactant micelles with a fluorescent probe, Austral. J. Chem. 29 (1976) 1-12.

[59 Oakes, Magnetic resonance studies in aqueous systems. Part 1.—Solubilization of spin probes by micellar solution, J. Chem. Soc., Faraday Trans. 2 68 (1972) 1464-1471.

[60 Goyal, B.A. Dasannacharya, V.K. Kelkar, C. Manohar, K. Srinivasa Rao, B.S. Valaulikar, Shapes and sizes of micelles in CTAB solutions, Physica B 174 (1991) 196-199.

[61 Durga Prasad, H.N. Singh, P.S. Goyal, K. Srinivasa Rao, Structural Transitions of CTAB Micelles in the Presence of n-Octylamine: A Small Angle Neutron Scattering Study, J. Colloid Interface Sci. 155 (1993) 415-419.

[62 Treiner, A,K. Chattopadhyay, R. Bury, Heat of Solution of Various Alcohols in Aqueous Micellar Solutions of Hexadecyltrimethylammonium Bromide as a Function of Surfactant Concentration: The Preferential Solvation Phenomenon, J. Colloid Interface Sci. 104 (1985) 569-578.

[63 Israelachvili, D.J. Mitchell, B.W. Ninham, Theory of Self-Assembly of Hydrocarbon Amphiphiles into Micelles and Bilayers, J. Chem. Soc., Faraday Trans. 2 72 (1976) 1525-1568.

[64 Bergstroem, I. Grillo, Correlation between the geometrical shape and growth behaviour of surfactant micelles investigated with small-angle neutron scattering, Soft Matter 10 (2014) 9362-9372.

[65 Kleber, H.-J. Bautsch, J. Bohm, I. Kleber, Einfuehrung in die Kristallographie, Verlag Technik Berlin, G.D.R., 1990.

[66 Almgren, V.M. Garamus, T. Asakawa, N. Jiang, Contrast Variation SANS Investigation of Composition Distribution in Mixed Surfactant Micelles, J. Phys. Chem. B 111 (2007) 7133-7141.

ACCEPTED MANUSCRIPT

[67 Rosenfeldt, N. Dingenouts, M. Ballauf, N. Werner, F. Voegtle, P. Lindner, Distribution of End Groups within a Dendritic Structure: A SANS study Including Contrast Variation, Macromolecules 35 (2002) 8098-8105.

ACCEPTED MANUSCRIPT